Meded. Zitt. K. Acad. Overzeese Wet.
Bull. Séanc. Acad. R. Sci. Outre-Mer
56 (2010-4): 437-456

Advancing Volcano Monitoring and Hazard Assessment in Africa through the Use of Remote Sensing Data: The Case Study of Oldoinyo Lengai, Tanzania*

by

Matthieu KERVYN**

KEYWORDS. — Volcanism; Monitoring; Hazard Assessment; Eruption; Remote Sensing; Oldoinyo Lengai.

SUMMARY. — Most volcanoes in developing countries are poorly studied and not regularly monitored. The present study aims at investigating how low-cost remote sensing data can be used to assess hazards and provide essential monitoring data for active volcanoes in Africa. We review here several applications specifically developed for the test case of Oldoinyo Lengai (OL), an active natrocarbonatite stratovolcano in North Tanzania, as an example of many other poorly known volcanoes. Satellite images enable the identification of three large sector collapses and the associated debris avalanche deposits which are dated to less than 10 ky. MODIS low spatial resolution images are used to monitor daily thermal emissions over eight years at OL, making it possible to illustrate the influence of earth tide cycle on the activity, and to document, in combination with field and petrological observations, the transition from effusive activity to large-scale explosive eruptions that took place in 2006 and 2007-2008. These results open new perspectives for the study of other active volcanoes in Africa (*e.g.* Rungwe, Virunga, Mt Cameroon).

MOTS-CLES. — Volcanisme; Surveillance; Analyse de risque; Eruption; Télédétection; Oldoinyo Lengai.

RESUME. — *Surveillance, analyse et prévision de l'aléa volcanique par télédétection en Afrique: l'exemple de l'Oldoinyo Lengai en Tanzanie*. — La majorité des volcans des pays en voie de développement sont peu étudiés ou irrégulièrement surveillés. Notre étude fait usage de données de télédétection à faible coût, combinées à des modélisations analogiques et numériques, pour identifier les risques et surveiller l'Oldoinyo Lengai, un stratovolcan natrocarbonatitique actif en Tanzanie, comme exemple de nombreux autres volcans peu connus. Les images satellites ont permis d'identifier et de modéliser trois effondrements de flanc et les avalanches de débris associées de moins de 10 000 ans. Des images MODIS à basse résolution spatiale ont également été utilisées pour surveiller pendant huit ans l'activité journalière du volcan, illustrer l'influence des cycles de marées terrestres sur son activité, et pour documenter, en combinaison avec des observations de terrain et des analyses pétrologiques, des éruptions effusives et explosives de grande ampleur,

* Paper presented at the meeting of the Section of Natural and Medical Sciences held on 27 April 2010. Publication decision taken on 22 February 2011. Final text received on 28 February 2011.

** Department of Geography, Vrije Universiteit Brussel, Pleinlaan 2, B-1050 Brussels (Belgium).

qui ont eu lieu en 2006 et 2007-2008, respectivement. Ces résultats ouvrent de nouvelles perspectives pour l'étude des autres régions volcaniques d'Afrique (ex. Rungwe, Virunga, Mt Cameroun).

Trefwoorden. — Vulkanisme; Monitoren; Risico analyse; Uitbarsting; Afstandwaarneming; Oldoinyo Lengai.

Samenvatting. — *Monitoren, analyse en voorspelling van vulkanische risico's door afstandwaarneming in Afrika: het voorbeeld van Oldoinyo Lengai in Tanzania.* — Veel vulkanen in ontwikkelingslanden worden niet bestudeerd of regelmatig opgevolgd. Onze studie maakt gebruik van goedkope afstandwaarnemingstechnieken, gecombineerd met analoge en numerieke modellen, om risico's te identificeren en om uitbarstingen te documenteren van Oldoinyo Lengai, een actieve natrocarbonatitische stratovulkaan in Tanzania, als een illustratief voorbeeld voor slecht gekende vulkanen. Satellietbeelden maken het mogelijk drie grootschalige flankinstortingen en geassocieerde puinlawine-afzettingen jonger dan 10 000 jaar te identificeren en te modelleren. Spatiale lage-resolutie MODIS-beelden werden gebruikt om de dagelijkse activiteit over acht jaar te monitoren, om de invloed van de aardgetijdencyclus op de activiteit aan te tonen, en om grootschalige effusieve en explosieve uitbarstingen die in 2006 en 2007-2008 plaatsvonden, in combinatie met veldgegevens en petrologische analyse, te bestuderen. Deze resultaten openen nieuwe perspectieven voor het bestuderen van de andere actieve vulkanische regio's in Afrika (bvb. Rungwe, Virunga, Mt Kameroen).

1. Introduction

Since the second half of the twentieth century, the science of volcanology has made significant progress, first through careful and systematic field observations, and then mostly through theoretical modelling and laboratory experimentation of volcanic processes, coupled with field work. More recently, integrated monitoring techniques, multidisciplinary research approaches, the increasing power of numerical computation, and the advent of remote sensing all have contributed to great advances in understanding volcanic processes. These pieces of research, however, focused on a limited number of volcanoes located in industrialized countries (*e.g.* Etna, Sicily, Italy or Kilauea, Hawaii, USA) or on volcanoes posing direct and important hazards to populations (*e.g.* Merapi, Indonesia).

Therefore these are mostly the same 200-300 volcanoes that have been mapped for topography, geology, volcanic hazards and risks and which are being continuously ground-monitored with state-of-the-art integrated techniques. These systematic studies have enabled the development of new monitoring techniques and provided a deeper understanding of processes at work at these volcanoes. This, however, leaves aside over two thirds of the ~1400 potentially active volcanoes which are poorly known and monitored (Simkin & Siebert 1994). Many of these potentially hazardous volcanoes are located in developing countries where the local systems struggle when it comes to assessing and mitigating volcanic hazards.

Volcanic hazards directly concern ~6 % of the world population (Tilling & Lipman 1993). They can indirectly affect a larger proportion of the world population through atmospheric-climatic or socio-economic effects, such as those which follow cataclysmic eruptions (*e.g.* 1815, Tambora — year without summer in 1816; 1883, Krakatoa; 1991, Mt Pinatubo) or moderately intense eruptions with large impacts on air traffic (2010, Eyjafjöll, Iceland). The rapidly increasing population living in developing countries is on average twenty times more vulnerable to natural disasters than in richer countries (measured as impact on GDP per head; World Bank website: www.worldbank.org).

So, there is an urgent need to gather basic knowledge about volcanoes' structures, potential range of eruptive styles and related hazards. There is also a need to adapt efficient and low-cost monitoring methods for those poorly studied volcanoes that represent a potential hazard for an increasing population. In this context, satellite remote sensing has the potential to make a significant contribution to advanced understanding of volcanoes and volcanic hazards at these poorly known volcanoes. This paper discusses how low-cost remote sensing data can be used and integrated with field data to monitor eruption intensity of poorly known volcanoes in Africa and elsewhere in the developing world and to assess hazards. This is done through the review of several applications developed for the specific case of Oldoinyo Lengai (OL) stratovolcano. The detailed description of this volcano and the applications here reviewed, are presented in more detail elsewhere (Kervyn *et al.* 2008a, b, c, 2010; Vaughan *et al.* 2008; Van Manen *et al.* 2010).

2. Oldoinyo Lengai and Associated Debris Avalanches

OL is a stratovolcano rising 2,000 m above the rift valley floor in North Tanzania (fig. 1). This is the only volcano on earth emitting natrocarbonatite lava. From 1983 to 2006, OL was almost continuously active with the activity being confined to small-scale effusive and explosive eruptions of natrocarbonatite within the summit crater. Natrocarbonatite lava is characterized by abnormally low temperature (~595°C, Krafft & Keller 1989) and viscosity (10^{-1} – 10^{2} Pa s, Norton & Pinkerton 1997) compared to silicic lava. A transition in eruptive style was observed at OL in 2006-2007 which culminated in a series of intense explosive eruptions of mixed magma composition, *i.e.* silicate and natrocarbonatite magma, in 2007-2008.

Remote sensing data were used to map and characterize in detail debris avalanche deposits originating from large sector collapses of OL, which were first documented in the field by Keller (2002) and Klaudius & Keller (2004). Field work provided evidence for volcano collapses and the presence of three major debris avalanche deposits of geologically young ages, *i.e.* younger than 10,000 yrs. Characterizing these debris avalanche deposits more closely using remote

sensing and a preliminary numerical modelling application helps better understand those collapse events that are now recognized as one of the major hazards at OL.

The remote sensing study of OL and the surrounding rift plain was carried out, using Digital Elevation Model (DEM) from the Shuttle Radar Topography Mission (SRTM), Landsat and ASTER imagery, available geological maps and aerial photographs. The SRTM DEM allowed the morphological characterization of OL and a reassessment of the volcano volume to 41 ± 5 km³. Multispectral and topographic remote sensing data interpretation enabled the mapping of the extent and the estimation of the volume of two sector-collapse scars and of three debris avalanche deposits (fig. 2). Debris avalanche deposits extend up to 24 km from OL; they cover 10 to 200 km² and have volumes estimated at 0.1 to ~5 km³, according to the respective average deposit thickness. Deposit surfaces were characterized by fields of large hummocks (>300 m across) and sharp edges typical of debris avalanche deposits.

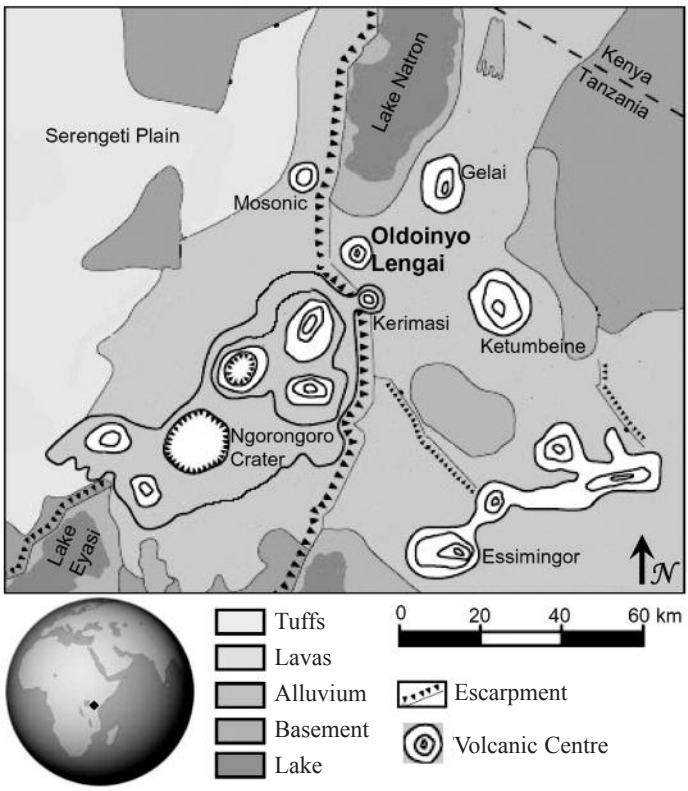

Fig. 1. — Location of Oldoinyo Lengai and regional geology (from Kervyn *et al.* 2008a, modified after Dawson 1992).

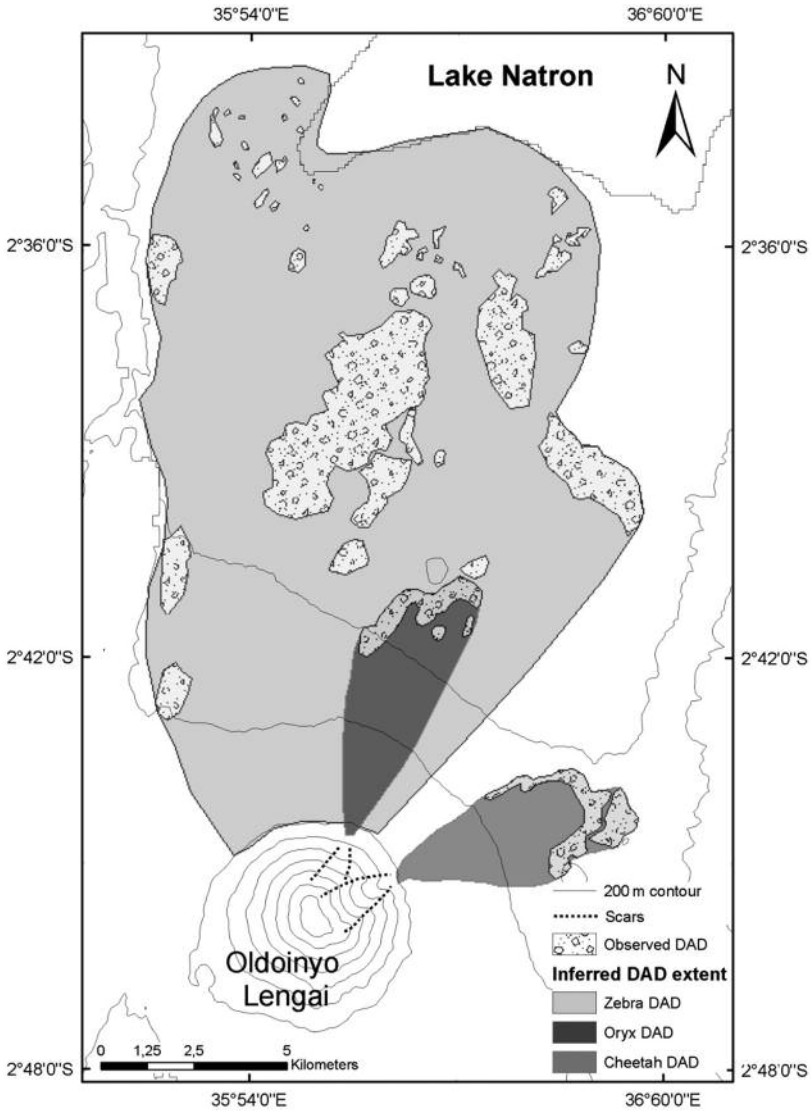

Fig. 2. — Outlines of three DADs originating from OL. The terrains with typical DAD morphology are individually delineated. The possible extent of the original DADs is extrapolated from the DAD terrain distributions, the morphology of the source zone and the surrounding topography.

One of the three avalanche events that occurred at OL is simulated by reconstructing the pre-avalanche volcano topography and the VOLCFLOW numerical model of Kelfoun & Druitt (2005) which is based on the depth-averaged granular flow equation and can account for different flow rheology. The best fit

model, which was run in MatLab, was obtained using a constant flow retarding stress of 45 kPa and contrasted internal (10°) and basal (3°) angles of friction. This simulation was able to reproduce the debris avalanche thickness distribution, the massive distal deposit front and the lateral levees. The simulation indicates initial flow velocities of the order of 100 m s^{-1}, distal velocities of 20-30 m s^{-1}, en-masse stoppage and emplacement in less than three minutes (fig. 3). The occurrence of young debris avalanche deposits around OL, up to 24 km distance, highlights the hazard related to catastrophic volcano flank collapses for the people, mostly Masai, who are living in the surrounding rift valley. Dramatic impact of such hazardous event can be mitigated only by the implementation of a routine monitoring of ground deformation and seismicity, using a combination of space-based (*e. g.* InSAR) and ground-based techniques (Calais *et al.* 2008).

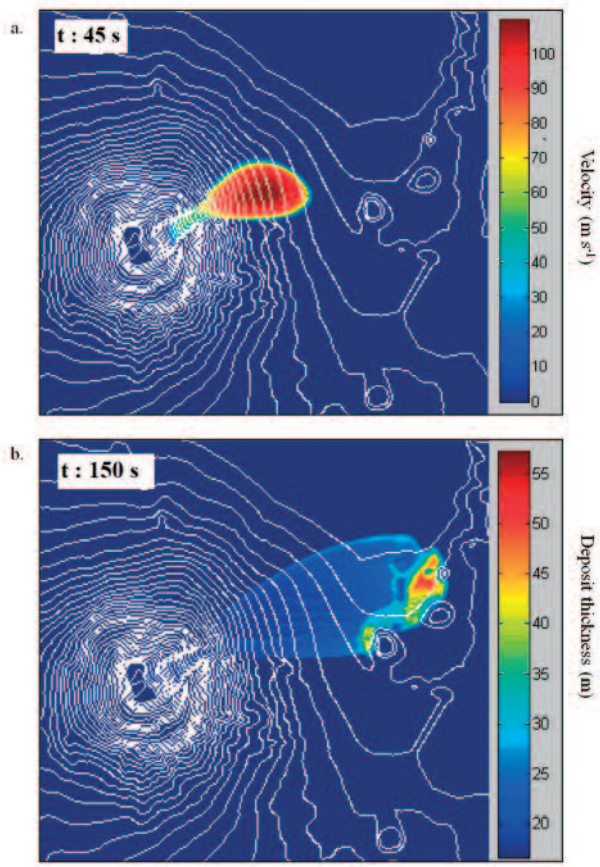

Fig. 3. — Numerical simulation of the eastern sector collapse of Oldoinyo Lengai with the model of Kelfoun & Druitt (2005): (a) flow velocity 45 s after intitiation of the collapse; (b) deposit thickness after 150 s when the avalanche comes to rest.

3. Methodology: An Algorithm to Detect Thermal Anomalies

Despite its near-continuous effusive activity and the expected transition to more explosive eruptions — which indeed occurred in 2007 — OL was not, and is still not, routinely monitored. This feature is common to all active volcanoes in Tanzania or Kenya. There is consequently an urgent need to develop a basic low-cost and remote monitoring system at OL, in order to document and investigate variations in the intensity of the eruptive activity. Using low spatial remote sensing images at 1 km spatial resolution acquired by the *Moderate Resolution Imaging Spectroradiometer* sensor (MODIS), a low-cost technique was developed with the aim of detecting the onset of any higher intensity eruptive episodes that could pose a threat for the local Masai people and for tourists.

First of all the capabilities of the existing automated MODVOLC algorithm, developed by Wright *et al.* (2002, 2004) to detect worldwide thermal anomalies, to monitor eruptive activity at OL were assessed. The identification of thermal anomalies by MODVOLC is based on a unique threshold of the Normalized Thermal Index (NTI), defined on night-time MODIS scene as:

$$NTI = \frac{R_{22} - R_{32}}{R_{22} + R_{32}} \qquad (1)$$

where R_{22} and R_{32} are radiance values derived from infrared band 22 (3.929-3.989 m) and thermal band 32 (11.770-12.270 m). Band 21 (3.929-3.989 m) is substituted for band 22 when the latter is saturated. Bands 21 and 22 saturate at pixel-integrated temperatures of approximately 500 K and 330 K, respectively. MODVOLC proved to fall short of detecting most thermal anomalies within OL's crater due to its small size compared to MODIS resolution (*i.e.* 10-10^3 m^2) and low temperature of OL lava flows (typically < 595 °C). Using field reports of eruptive activity and higher resolution satellite images (ASTER, Landsat ETM+) as calibration data, we explored how MODIS infrared bands could still be used to monitor OL activity by adapting and calibrating the MODVOLC algorithm to the specific characteristics of OL eruptions.

The MODLEN therefore adapted to the MODVOLC approach by:

— Extracting a subscene from each image centred on the OL summit;
— Using a NTI threshold value specifically adapted to OL (threshold = - 0.88);
— Setting a spatial derivative threshold to identify whether a pixel is thermally anomalous relative to the immediate neighbouring pixels (Kervyn *et al.* 2008a);
— Automatically recording radiance values for the pixel covering OL summit even in the absence of a thermal anomaly, in order to define a comparison baseline and to enable the assessment of cloud coverage influence.

Comparison of MODLEN results with field observations allowed the validation of the MODLEN to detect low-intensity eruptive activity at OL (fig. 4). All

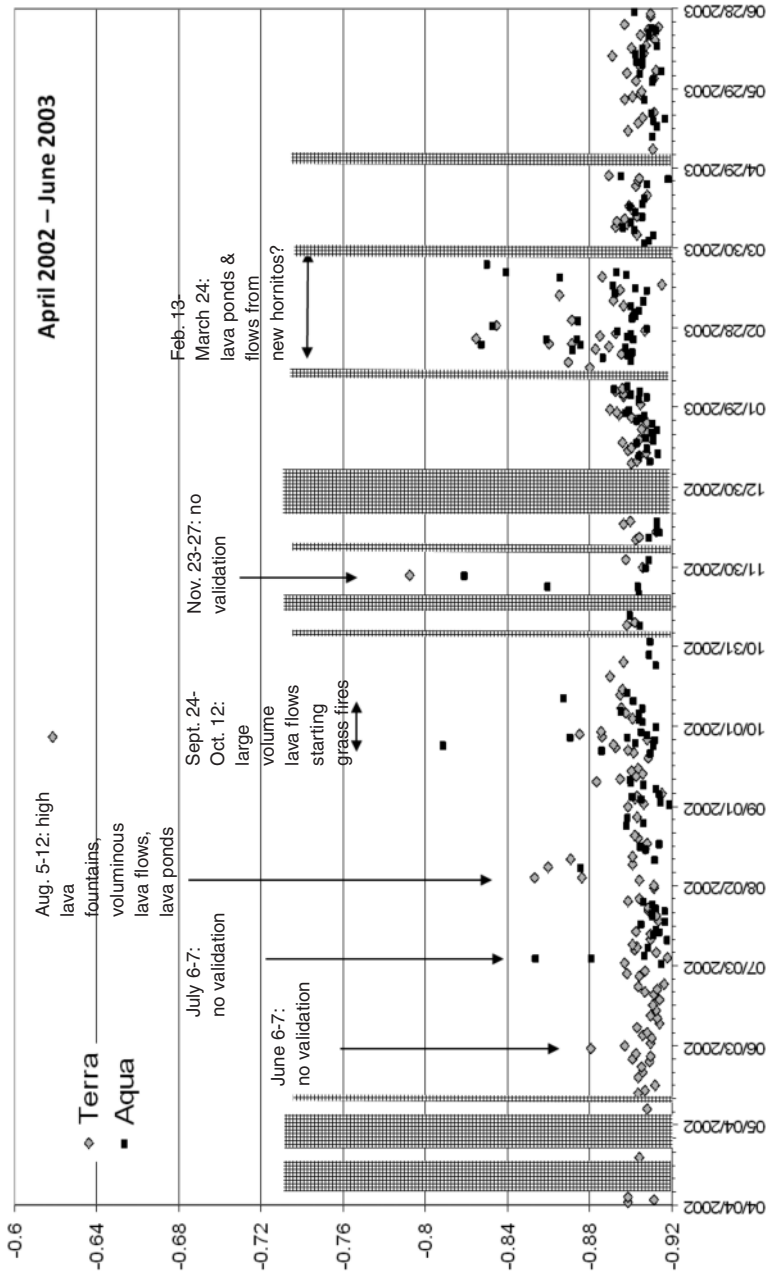

Fig. 4. — Example of time-series data from April 2002 to June 2003 of the Normalized Thermal Index (NTI). Plotted are cloud-free MODIS night-time scenes for pixels covering OL summit, and hotspot pixels detected by MODLEN within 2 km of OL summit. Periods for which data are lacking (*i.e.* due to cloud coverage or satellite data acquisition gaps) for more than five consecutive days, are marked by grey vertical bars. Detailed field reports exist only for the end of June and the first days of August 2002 as discussed in the text

night-time MODIS scenes acquired by two instruments, one flown on the Terra and one on the Aqua satellite between February 2000 and March 2008, were analysed using the MODLEN algorithm (Kervyn *et al.* 2008a, c, 2010; Vaughan *et al.* 2008; Van Manen *et al.* 2010). Figure 5 illustrates the temporal distribution and relative intensity of all thermal anomalies with a NTI > - 0.88.

MODLEN data has four drawbacks for monitoring purposes (Kervyn *et al.* 2008a):

— The limited time slot of acquisition, data being only acquired between 19:30 and 23:40 daily;
— The frequent cloud coverage preventing detection of thermal anomalies, especially during the rainy season from November to March;
— The detection of non-volcanogenic thermal anomalies such as bush fires, although, these can be discriminated in the data set through the calculation of the distance between the anomalous pixel and OL summit.

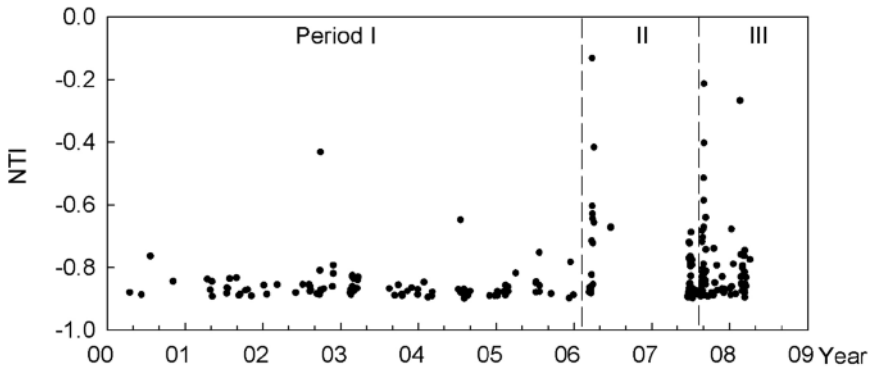

Fig. 5. — NTI values of the detected anomalies from 2000-2008, identifying three separate periods of activity as defined in the text.

4. Results

4.1. Temporal Distribution of Eruptive Activity

More than 4,100 night-time MODIS scenes acquired by Aqua and Terra satellites between February 2000 and February 2008 were downloaded and analysed by using the MODLEN algorithm. Over this period MODLEN enabled to detect 297 thermal anomalies at OL summit, suggesting moderate-to-intense eruptive activity on 213 different satellite scenes covering 157 different days (fig. 5). So, MODLEN detected at least one alert on ~8 % of the days for which a cloud-free scene was available (*i.e.* ~30 % of the data being affected by cloud coverage).

This relatively low percentage about the reported eruptive activity at OL is attributed to the fact that OL's lava flows erupt at a temperatures of ca. 495-595 °C (Krafft & Keller 1989, Dawson *et al.* 1990, Pinkerton *et al.* 1995). Activity needs to be four times as spatially extensive as for a basaltic flow (at 1,200 °C) to produce a similar thermal radiance at the wavelengths of MODIS bands 21 and 22 (Kervyn *et al.* 2008a).

An independent data set compiled from the field reports for the 209 days for which activity has been observed from the ground since 2001 allows assessment of the frequency of activity at OL. This compilation indeed suggests that "no activity" or "weak open vent/lava pool degassing" has been observed on 44 % of the days. On 50 % of the days low to moderate eruptive activity was recorded (tens of metres long lava flows within the crater and strombolian activity). High-intensity activity, including high volume sustained flows, high lava fountains, and ash explosions, were observed for only 6 % of the observation days. This suggests that MODLEN is mostly sensitive to high intensity eruption events at OL.

The comparison with field observations therefore suggests that MODLEN is capable of identifying virtually all periods of intense eruptions, especially those related to large active lava pools and extensive lava flow activity or hot pyroclastic deposits that were detected during explosive episodes in 2007 and 2008. Fumaroles, Strombolian activity and small lava flows are unlikely to be detected in the 1 km-MODIS pixels, due to their low temperatures and rapid cooling. Detection of Strombolian activity is only likely if activity is coincident with the satellite overpass.

Figure 4 illustrates the NTI values for a fifteen-month-long period between April 2002 and June 2003. The thermal time series shows a dominant low, baseline, level within which a low amplitude seasonal effect is apparent, with slightly higher values in September-October and February-March when the sun is at its highest elevation at this latitude. Such seasonal variation of the baseline was observed by Dehn *et al.* (2000) for the North-Pacific volcanoes. A total of twenty-seven MODLEN alerts were detected over this period. An additional ten pixels are visually identified as anomalous due to their above-mentioned baseline values in the thermal time series. These were not flagged as alerts because they were adjacent to a high intensity hot spot or were just below the - 0.88 threshold. These alerts occur in six main periods each lasting from a couple of days to a month (fig. 5).

MODLEN is able to detect eruptive events that were not witnessed on the ground because of low human presence within the area (*e.g.* June 2 and July 6-7, 2002) and to constrain more accurately events for which incomplete information is available. This is the case for the event at the end of September 2002. Eruptive activity at OL was eyewitnessed for two hours on September 26 when several active flows, as well as many inactive but recent flows, were identified (GVN 2002). A grass fire was observed on the volcano NW flank on the following day. This report corresponds to a nineteen-day-long eruption period recorded by

MODLEN in September and October 2002. MODLEN identified eleven alert pixels on September 27 on the N flank, consistent with the observations of a fire started by lava flowing over the crater rim. Poorly detailed reports of the growth of new *hornitos* during the first half of 2003 are consistent with MODLEN results that display a six-week-long period of high activity from February 13 to March 24, 2003. On the other hand, low level activity, such as on June 18, 2002 when vent spattering reached heights of up to 3 m and produced a 50 m-long lava flow (GVN 2002), are not systematically detected by MODLEN.

Although the continuity of the MODIS data in the rainy seasons (*i.e.* November-December and March-May) is affected by frequent cloud coverage, a high intensity eruption period is clearly identified by MODLEN during the last week of November 2002, with three MODLEN alerts on November 23 and 27, 2002, (fig. 4). One of these alerts was detected when the volcano was unambiguously cloud-covered. This shows that a strong thermal anomaly can still be detected, even through thin or broken clouds.

Periods of detected thermal activity at OL vary from a single scene to repeated thermal anomalies detected over a period of thirty-seven days. Periods of prolonged activity (*i.e.* over one week) have been detected especially in February-March, July and September-October. The time series from February 2000 to the end of 2005, before the changes in eruption style (see section 4.3), show characteristic time intervals between successive alerts. 33 % of active days are separated by less than five days. The frequency of longer time intervals decreases exponentially. Some intervals are however more frequent than expected from this simple trend, especially ten to fifteen, twenty-five to thirty and fifty-one to sixty days.

When the temporal distribution of detected activities between 2000 and 2005 is analysed throughout the year, it appears that there are two main periods of activity (fig. 6a). There is a first, short and well-defined peak of activity in February-March, followed by a drastic decrease in the frequency of eruptive events between April and June. July marks a second peak in the frequency of intense eruptive events, the frequency of events decreasing gradually until October. There is a smaller peak of activity in November. Although the availability of cloud-free images throughout the year is not constant, weighting the raw observations by the number of available cloud-free scenes per month does not change the observations, the February-March and November peaks being even more pronounced as they fall within the rainy seasons during which less cloud-free scenes are available. Interestingly, the overall monthly distribution of detected days of activity from 2006 to February 2008 is not much different from the previous period, despite significant changes in eruptive behaviour (fig. 5). In 2006, most anomalies occurred in March whereas in 2007, MODLEN detected many thermal hot spots from end of June to early September, before the onset of the explosive eruptions (Vaughan *et al.* 2008).

The monthly distribution of intense eruptive events extracted for the 414 days for which field reports are available since 1987 has provided similar information

as MODLEN. The proportion of days with low to moderate activity is rather constant throughout the years, with lower values in January and a marked peak in November. The distribution of the high intensity events resembles that obtained with the MODLEN data, with a marked peak in June-July and decreasing activity occurrence afterward. The uneven distribution of field observations throughout the year, with few observations during the rainy seasons, limits the validity of this analysis.

4.2. Environmental Controls on Eruptive Activity

Empirical observations at OL suggest that variations of eruption intensity, or eruption rate, are not random with time. Recent field work has been dedicated to test the hypothesis that the eruption rate at OL is controlled by daily earth tides, atmospheric pressure and/or moon cycles. Based on hourly observations for a thirty-day-long period at OL's summit in July 2004, a statistically significant positive correlation was observed for that period between increasing volcanic activity and decreasing or minimum barometric pressure (Gordon *et al.* 2005). Analysis of the same observations against earth tide cycles indicated no correlation between activity and the diurnal tidal cycles. Analysis, however, suggested activity cycles with periods of 8.5 days and 30 hours, respectively (Gordon *et al.* 2005).

Such analysis is based on the hypothesis that the control of environmental factors, such as earth tides and barometric pressure on eruption rate and activity, might be more pronounced at OL than at other volcanoes due to its low magma viscosity and to the open nature of its magmatic system. The 2000-2005 MODLEN time series offers a unique opportunity to test the potential controls of these environmental factors on the temporal distribution of activity at OL. One objective of this analysis is to assess if the uneven distribution of activity throughout the year can be attributed to external forces or if it is related to internal characteristics of the OL magmatic system.

Theoretical earth tides were computed by using TSOFT software, which was developed by the International Centre for Earth Tides in Brussels (Van Camp & Vauterin 2005). The maximum tide amplitude and minimum/maximum tide values (*i.e.* in nm s^{-2} as tide is an acceleration) were computed for each day of the six-year time series. The timings of the maximum tide amplitude and of the minimum/maximum tidal acceleration are the parameters that are thought to exert a possible influence on the eruption intensity. The field and MODLEN data are not sufficient to allow for analysis at the hour scale, so relationships between eruptive activity and earth tides are analysed at the scale of fourteen-day cycles, according to the position and declination of the moon relative to the Earth, and of semi-annual cycles, associated with the Earth rotation around the sun.

The temporal distribution of eruptive activity appears to be strongly correlated with the semi-annual variation of earth tides. Figure 6b illustrates the number

of days between each day of detected activity and the closest semi-annual earth tide amplitude maximum. This graph shows that a majority of the activity (64 %) occurs within seventy days prior to earth tide amplitude maximum, with the highest frequencies being recorded twenty to thirty and fifty to sixty days before the tide maximum amplitude. Only 25 % of the activity occurs after the earth tide amplitude maximum. This suggests that the gradually increasing amplitude of earth tides, and thus the gradually higher negative acceleration effect caused by tides, over a six-month period, tends to favour intense activity at OL. High intensity eruptions observed in the field also occurred thirty to eighty days before an earth tide maximum, even though the uneven distribution of observations relative to the date of the earth tide maxima gives little significance to this last observation.

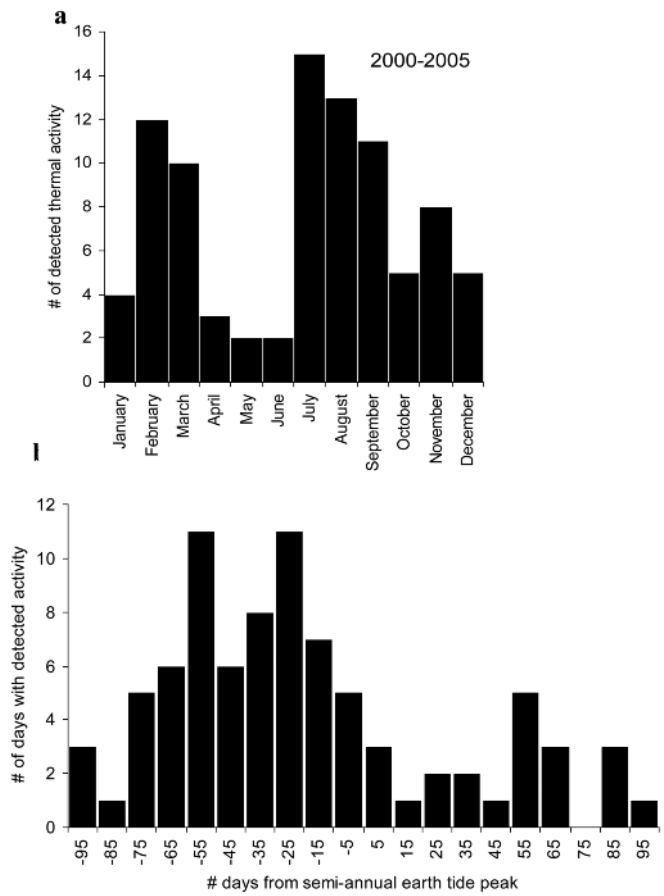

Fig. 6. — Temporal distribution of the eighty-five days for which thermal activity was detected by MODLEN from 2000 to 2005: (a) number of days of activity per month of the year; (b) distribution of the detected days of activity relative to the semi-annual earth tide amplitude maxima.

The characteristic time interval between MODLEN alerts suggests that a monthly (*i.e.* ~28 days) and/or a half monthly (*i.e.* ~14 days) cycle controls part of the temporal distribution of activity at OL. Time intervals of ten to fifteen and twenty-five to thirty days are indeed more frequent than other values. The analysis of the number of days between each day of activity and the closest fourteen days amplitude maximum does not, however, return a clear trend. The frequency of activity is observed to increase when approaching the earth tide amplitude maximum but high frequencies of activity are also observed five to seven days after that peak. Van Manen *et al*. (2010) also called for caution in using the MODIS thermal anomalies to infer environmental controls on the temporal distribution of eruptive activity, even at the half-year scale, due to significant statistical artefacts affecting the data associated with the non-random temporal distribution of MODIS acquisition and to the effect of cloud coverage, preventing the identification of all potential thermal anomalies.

Annual variation in barometric pressure in North Tanzania can also account for part of the annual variations in eruption intensity. Every year, the atmospheric pressure reaches a maximum around the end of June and a minimum between late November and late February. The drop in pressure after the June peak is nicely correlated with the onset of increased activity at OL in July. The decrease in atmospheric pressure might thus play a role in the opening of ground fractures that enable the pressurized magma to reach the surface. Similar mechanisms associated with seasonal Earth surface deformation have been postulated to control seasonal variation of volcanic activity over entire regions by Mason *et al.* (2004).

In conclusion, field and MODIS observations of activity at OL suggest that moderate-to-intense eruptive events occur more frequently when earth tide amplitude is increasing and when atmospheric pressure is decreasing on a year-long timescale, although the current data set is not sufficiently robust for these correlations to be statistically significant. This effect of environmental factors is probably enhanced at OL by the low viscosity of its magma and the fact that magma is stored in shallow magma reservoirs (Pyle *et al.* 1995) related to the surface through open conduits. Other environmental parameters might also influence eruptive activity, such as rainfalls. Mason *et al.* (2004) indeed proposed that the seasonal variation in activity can be correlated with the soil humidity and other variations of the hydrological system, causing variations in the crust elevation. For the case of OL, the timing of the two rainy seasons (November to mid-December and March to May) does not show direct correlation with distribution of eruptive events. One should also keep in mind that the timing of successive eruptive events, especially the most voluminous ones, is probably also constrained by characteristics of the magmatic system, mainly the magma supply rate to the shallow magma reservoirs.

In order to enable a better understanding of the role of environmental factors and to test the influence of these effects at shorter (*i.e.* hour to day-scale) and

longer (*i.e.* 4.65 and 18.6 years earth tide cycles) timescales, there is a need to collect continuous and quantitative observations of the activity at OL. This could be achieved by installing an infrared camera, or an optical webcam to start with, at the summit of OL, to provide continuous observation of the eruptive activity.

4.3. Transition in Eruptive Dynamics

This thermal remote sensing monitoring system was developed a few months prior to a significant change in eruptive style at OL. The first stage of this transition was marked by a large effusive eruption from March 25 to April 5, 2006, which produced the largest natrocarbonatite lava flow ever documented at OL, in two main phases. It was associated with the collapse of several of the *hornitos* in the active crater, rapid extrusion of magma stored in shallow reservoirs causing flooding of a third of the crater floor and development of a 3 km-long compound rubbly *pāhoehoe* to blocky *ʻaʻā*-like flow on the west flank. The eruption was followed by rapid enlargement of a pit crater (fig. 7a). The erupted natrocarbonatite lava had a higher than usual silica content (3 % SiO_2 as compared to < 0.3 % for typical natrocarbonatite lava). The eruption chronology was reconstructed from eyewitness and news media reports and MODLEN data, which provided the most reliable evidence to constrain the eruption's onset and variations in activity. The eruption products were mapped in the field and the total erupted lava volume estimated at $9.2 \pm 3.0 \times 10^5$ m^3, a volume equivalent to the yearly magma output rate between 1983 and 2005 at OL. The event chronology from remote sensing and the field evidence suggested that two phases of vent construct collapse caused magma mixing and rapid extrusion from shallow reservoirs (Kervyn *et al.* 2008c).

Natrocarbonatite eruptions resumed by June 2007 after a year-long hiatus in activity since the 2006 lava flow. Through July and August 2007, over twenty-five tectonic earthquakes of magnitude 4 to 5.9 on the Richter scale were reported within 50 km of OL. This seismic crisis, which was originally attributed to eruptive activity at OL, was later shown to result from a voluminous dyke intrusion into the flank of Gelai volcano, 15 km north-west of OL (Calais *et al.* 2008). The relationship between this intrusion and the onset of explosive activity at OL a few weeks later remains a matter of debate (Calais *et al.* 2008, Kervyn *et al.* 2010).

On September 4, 2007, after twenty-five years of effusive natrocarbonatite eruptions, the eruptive activity of OL changed abruptly to episodic explosive eruptions. The eruption was initially characterized by 2-3 km high ash columns. It caused damage to vegetation on the volcano slopes, ash fallout to at least 20 km from OL's summit and self-evacuation of several Masai villages. After the opening phase, the activity continued for eight months, varying from 100 m high ash jets to 2-15 km high violent, steady or unsteady, eruption columns dispersing ash to 100 km distance. The explosive eruptions built up a ~400 m wide, ~75 m high intracrater pyroclastic cone (fig. 7c).

Fig. 7. — Evolution of Oldoinyo Lengai crater morphology viewed from north: (a) in June 2006; (b) early September 2007; (c) March 2008 (photo courtesy: Benoît Wihelmi).

Despite the lack of ground-based monitoring, the evolution in OL eruption dynamics could be documented basing on the available field observations, ASTER and MODIS satellite images, and almost daily photos provided by local aircraft pilots (fig. 7b, c). Satellite data enabled identification of a phase of voluminous lava effusion in the two weeks prior to the onset of explosive eruptions. Spectral analysis of an ASTER image acquired the first day of the eruption provided the first evidence for a silicate composition of the ash cloud (Vaughan *et al.* 2008). Time-series data for eruption column height showed distinct peaks at the end of September 2007 and February 2008, the latter being associated with the first pyroclastic flows to be documented at OL (Kervyn *et al.* 2010). Chemical analyses of the erupted products show that the 2007-2008 explosive eruptions are associated with an undersaturated carbonated silicate melt (Keller *et al.* 2010).

Remote sensing proved again to be an essential source of information to detect the early stage of the transition from effusive activity to explosive eruptions and to follow the day-to-day variation in eruption intensity and behaviour. Early detection of the increased thermal emission at the end of August 2007 and rapid detection on ASTER image of the onset of the explosive eruption enabled us to disseminate essential information regarding associated hazards to the local actors of the tourism industry and to Tanzanian geologists in charge of managing such hazard. Due to the remoteness of OL and the absence of ground-based monitoring, the combination of satellite images at contrasted spatial and temporal resolution with available airphotos offered a unique way to document this unusual eruption and to gain new insights into the evolution of the shallow magmatic system at this unique natrocarbonatite volcano.

5. Conclusions and Perspectives

This paper highlights the advantages of low-cost remote sensing data sets to assess hazards and monitor active volcanoes in developing countries. It shows the value of combining complementary remote sensing data sets with limited available field data to make significant advances in the understanding of a volcano and to gain insights into the hazards associated with its eruptive activity.

Multispectral satellite data, SRTM DEM and airphotos confirmed the existence and permitted mapping, characterization of surface morphology and quantitative estimation of the volume of three debris avalanche deposits at OL. Use of high temporal and low spatial resolution MODIS data analysed with an adapted algorithm (MODLEN) enabled to document eruptive activity at OL for the last eight years (Kervyn *et al.* 2008a). This is the first time an active volcano in Africa is continuously monitored for several years, providing baseline knowledge of its eruptive behaviour. MODLEN data allowed to identify and characterize the transition from regular natrocarbonatite activity to voluminous effusive eruptions

(KERVYN *et al.* 2008c) and then to explosive eruptions (VAUGHAN *et al.* 2008). Temporal analysis of this time series also enabled to highlight the possible influence of external forcings such as earth tides on the occurrence of high intensity activity at this open magmatic system characterized by a low viscosity melt.

At the end of 2007, OL changed its style of activity to episodic explosive eruptions. Ash from these subplinian-style eruptions adversely affected the local Masai population, prohibited access to the volcano for tourists and caused disruption of the local air traffic. Despite the changing character of the eruptive activity at OL and the risk it represents for the increasing amount of tourists climbing OL each year, there is dramatic lack of geophysical data (*e.g.* seismic or ground deformation), of continuous gas monitoring data, of systematic field observations or product sampling at OL. As illustrated by the applications reviewed above, an integrated analysis of available sources of remote sensing data makes it possible to still provide timely assessment of evolving hazards by identifying and characterizing the intensity of thermal and ash emissions, by retrieving the dominant composition of erupted ash and potentially the eruption column height, as well as by detecting the occurrence of pyroclastic flows at OL.

One objective of this research was to identify low-cost solutions adapted to the specific circumstances in developing countries. These include the lack of training in remote sensing and in modelling hazards, lack of computer resources, lack of high-resolution topographic data sets and the limited access to satellite imagery or topographic data restricted to free images available on internet (ERNST *et al.* 2008). The low-cost approaches developed here to monitor low-level thermal activity over extended periods of time and to document and model flank collapses could be applied at some of the many volcanoes that have not been accurately mapped or studied for their hazards and monitored with state-of-the-art techniques, including active and potentially active volcanoes across Africa. The remote sensing data and the methods used should be adapted to the type of volcanic activity and the expected hazards. In this way, remote sensing has the potential to enable rapid hazard assessment and basic remote monitoring at many volcanoes.

There is therefore a need to share advances in remote sensing of volcanoes with scientists in developing countries and to help them build up the facilities needed to develop research on the many volcanoes that have yet to be studied. Mapping and assessing hazards in high-risk areas in advance of an eruptive crisis and educating local communities about the volcano-related hazards, can help mitigate the adverse impacts of future eruptions.

ACKNOWLEDGEMENTS

The work presented here was the subject of a lecture before the Royal Academy for Overseas Sciences on April 28, 2010. This is the result of my PhD research developed at the University of Ghent funded by the *Fonds voor Wetenschappelijk Onderzoek* –

Vlaanderen. I am grateful to Gerald G. J. Ernst and Prof. P. Jacobs, my PhD supervisors, for initiating the research on African volcanism at UGent and for the discussions about my research. The results presented here benefited from collaborations and fruitful discussions with Belgian and international scientists, including K. Fontijn, A. Harris, J. Keller, E. Mbede, G. Vaughan, S. Van Manen, F. Kervyn and many others. The help of Majura Songho in the field was greatly appreciated.

REFERENCES

Calais, E., d'Oreye, N., Albaric, J., Deschamps, A., Delvaux, D., Deverchere, J., Ebinger, C., Ferdinand, R. W., Kervyn, F., Macheyeki, A. S., Oyen, A., Perrot, J., Saria, E., Smets, B., Stamps, D. S. & Wauthier, C. 2008. Strain accommodation by slow slip and dyking in a youthful continental rift, East Africa. — *Nature*, **456**: 783-787.

Dawson, J. B. 1992. Neogene tectonics and volcanicity in the North Tanzanian sector of the Gregory Rift Valley: Contrasts with the Kenya sector. — *Tectonophysics*, **204**: 81-92.

Dawson, J. B., Pinkerton, H., Norton, G. E. & Pyle, D. M. 1990. Physicochemical properties of alkali carbonatite lavas: Data from the 1988 eruption of Oldoinyo Lengai, Tanzania. — *Geology*, **18**: 260-263.

Dehn, J., Dean, K. & Engle, K. 2000. Thermal monitoring of North Pacific volcanoes from space. — *Geology*, **28**: 755-758.

Ernst, G. G. J., Kervyn, M. & Teeuw, R. M. 2008. Advances in the remote sensing of volcanic activity and hazards, with special consideration for applications in developing countries. — *Int. J. Remote Sensing*, **29**: 6687-6723.

Gordon, J., Belton, F., Cribb, W. & Henry, J. 2005. Influences of changing lunar cycle and barometric pressure on the eruption of natrocarbonatite lava, Ol Doinyo Lengai volcano, Tanzania. — *Geological Society of America Abstracts with Programs*, **37**: 7.

GVN 2002. Oldoinyo Lengai: Lava exits crater at 3 points during January 2001-September 2002. — *Bull. Global Volc. Network*, **27** (10): ???:

Kelfoun, K. & Druitt, T. H. 2005. Numerical modeling of the emplacement of Socompa rock avalanche, Chile. — *J. Geophys. Res*., **110**: doi:10.1029/2005JB003758.

Keller, J. 2002. Cone collapses, flank stability and hazards at Oldoinyo Lengai, Tanzania. — *In*: IAVCEI International Congress Abstracts with Program, Montagne Pelée 1902-2002, p. 68.

Keller, J., Klaudius, J., Kervyn, M. & Ernst, G. G. J. 2010. Fundamental changes in the activity of the natrocarbonatite volcano Oldoinyo Lengai, Tanzania: I. New magma composition. — *Bull. Volcanol*., **72**: 893-912.

Kervyn, M., Ernst, G. G. J., Harris, A. J. L., Belton, F., Mbede, E. & Jacobs, P. 2008a. Thermal remote sensing of the low-intensity thermal anomalies of Oldoinyo Lengai, Tanzania. — *Int. J. Remote Sensing*, **29**: 6467-6499.

Kervyn, M., Ernst, G. G. J., Klaudius, J., Keller, J., Mbede, E. & Jacobs, P. 2008b. Remote sensing evidence for sector collapses and debris avalanches at Oldoinyo Lengai and Kerimasi volcanoes, Tanzania. — *Int. J. Remote Sensing*, **29**: 6565-6595.

Kervyn, M., Ernst, G. G. J., Klaudius, J., Keller, J., Kervyn, F., Mattsson, H. B., Betlon, F., Mbede, E. & Jacobs, P. 2008c. Voluminous lava flows at Oldoinyo Lengai in 2006: Chronology of events and insights into the shallow magmatic system of a natrocarbonatite volcano. — *Bull. Volcanol*., **70**: 1069-1086.

Kervyn, M., Ernst, G. G. J., Keller, J., Vaughan, R. G., Klaudius, J., Pradal, E., Belton, F., Mattsson, H., Mbede, E. & Jacobs, P. 2010. Fundamental changes in the activity of the natrocarbonatite volcano Oldoinyo Lengai, Tanzania: II. Eruptive behaviour. — *Bull. Volcanol*., **72**: 913-931.

Klaudius, J. & Keller, J. 2004. Quaternary debris avalanche deposits at Oldoinyo Lengai (Tanzania). — *In*: IAVCEI General Assembly Abstracts with Program, Pucon, Chile.

Krafft, M. & Keller, J. 1989. Temperature measurements in carbonatite lava-lake and flows: Oldoinyo Lengai, Tanzania. — *Science*, **245**: 168-170.

Mason, B. G., Pyle, D. M., Dade, W. B. & Jupp, T. 2004. Seasonality of volcanic eruptions. — *J. Geophys. Res*., **109**: doi: 10.1029/2002JB002293.

Norton, G. E. & Pinkerton, H. 1997. Rheological properties of natrocarbonatite lavas from Oldoinyo Lengai, Tanzania. — *Eur. J. Mineral*., **9**: 351-364.

Pinkerton, H., Norton, G. E., Dawson, J. B. & Pyle, D. M. 1995. Field observations and measurements of the physical properties of Oldoinyo Lengai alkali carbonatite lavas, November 1988. — *IAVCEI Proc. Volcanol*., **4**: 23-36.

Pyle, D. M., Pinkerton, H., Norton, G. E. & Dawson, J. B. 1995. The dynamics of degassing at Oldoinyo Lengai. — *IAVCEI Proc. Volcanol*., **4**: 37-46.

Simkin, T. & Siebert, L. 1994. Volcanoes of the World. — Tucson, Geosciences Press, p 349.

Tilling, R. I. & Lipman, P. W. 1993. Lessons in reducing volcano risk. — *Nature*, **364**: 277-280

Van Camp, M. & Vauterin, P. 2005. Tsoft: Graphical and interactive software for the analysis of time series and Earth tides. — *Comput. Geosci*., **31**: 631-640.

Van Manen, S., Kervyn, M., Blake, S. & Ernst, G. G. J. 2010. Apparent tidal influence on thermal activity at Oldoinyo Lengai volcano, Tanzania, as observed in Moderate Resolution Imaging Spectroradiometer (MODIS) data. — *J. Volcanol. Geotherm. Res*., **189**: 151-157.

Vaughan, R. G., Kervyn, M., Realmuto, V., Abrams, M. & Hook, S. J. 2008. Satellite measurements of recent volcanic activity at Oldoinyo Lengai, Tanzania. — *J. Volcanol. Geotherm. Res*., **173**: 196-206.

Wright, R., Flynn, L., Garbeil, H., Harris, A. & Pilger, E. 2002. Automated volcanic eruption detection using MODIS. — *Remote Sensing of Environment*, **82**: 135-155.

Wright, R., Flynn, L. P., Garbeil, H., Harris, A. J. L. & Pilger, E. 2004. MODVOLC: Near-real-time thermal monitoring of global volcanism. — *Journal of Volcanology and Geothermal Research*, **135**: 29-49.